Available online on 15.02.2019 at http://jddtonline.info

Journal of Drug Delivery and Therapeutics

Open Access to Pharmaceutical and Medical Research

Open Access Research Article

Solanum tuberosum extract mediated synthesis and characterization of iron oxide nanoparticles for their antibacterial and antioxidant activity

Madhu GC[1], Jaianand Kannaiyan[2], Rameshkumar K[3], Eyini Muthukumarasamy[4], Balaji Paulraj[2], Veeramanikandan Veeramani[1*]

[1] PG & Research Centre in Microbiology, MGR College, Dr. MGR Nagar, Hosur, Tamil Nadu, India

[2] PG & Research Centre in Biotechnology, MGR College, Dr. MGR Nagar, Hosur, Tamil Nadu, India

[3] PG and Research Department of Zoology, Vivekananda College, Madurai, Tamilnadu, India

[4] Centre for Research and PG studies in Botany, Thiagarajar College, Madurai, Tamilnadu, India

ABSTRACT

In the present study, the potential of aqueous extract of *Solanum tuberosum* for synthesis of Iron Oxide nanoparticles (Fe_3O_4) was evaluated. An eco-friendly synthesis of iron oxide nanoparticles and characteristics of the obtained Fe_3O_4 nanoparticles were studied using Ultraviolet-visible spectroscopy (UV-Vis), Fourier Transform Infra-Red Spectroscopy (FTIR), Scanning Electron Microscope (SEM), Energy-dispersive X-ray spectroscopy (EDX), X-Ray Diffraction (XRD) and High Performance Liquid Chromatography (HPLC). The synthesized Iron oxide nanoparticles were effectively utilized for the antibacterial activity and antioxidant studies. The rapid biological synthesis of iron oxide nanoparticles using the extract of *S. tuberosum* provides an environment friendly, simple and efficient route. From the results, it is suggested that synthesized Iron Oxide could be used effectively in future biomedical engineering.

Keywords: Antibacterial, Antioxidant, Iron oxide (Fe_3O_4) nanoparticles, *Solanum tuberosum.*

Article Info: Received 05 Dec 2018; Review Completed 18 Jan 2019; Accepted 20 Jan 2019; Available online 15 Feb 2019

Cite this article as:

Madhu GC, Jaianand K, Rameshkumar K, Eyini M, Balaji P, Veeramanikandan V, *Solanum tuberosum* extract mediated synthesis and characterization of iron oxide nanoparticles for their antibacterial and antioxidant activity, Journal of Drug Delivery and Therapeutics. 2019; 9(1-s):5-15 **http://dx.doi.org/10.22270/jddt.v9i1-s.2238**

***Address for Correspondence:**

Dr. Veeramanikandan Veeramani, Assistant Professor, Research Centre in Microbiology, MGR College, Dr. M.G.R. Nagar, Hosur- 635 109, Tamilnadu, India

INTRODUCTION

The synthesis of nanomaterials and the investigation of their possessions and uses is one of the interesting parts in the current scientific research. Researchers have shown extreme interest to discover various remarkable structures of nanoparticles. Such nanomaterials have developing application in numerous practical fields including biomedical, catalysis, biosensors and energy storage devices. The main purpose behind the intense significance of nanoparticles is the exposure of many storage and concealed features at the nanoscale[1, 2, 3]. Nanoparticles synthesis is presently an important area of investigation, searching for an eco-friendly approach for present situation.

Solanum tuberosum belonging to the family Solanaceae include a number of commonly collected or cultivated species. The major species grown worldwide is *Solanum tuberosum* (a tetraploid with 48 chromosomes), and modern varieties of this species are the most widely cultivated[4]. Due to the presence of active constituent, plant has been reported to possess various pharmacological activities such as antibacterial, antifungal, antitumor, hypotension effect etc. The aim of the work presented here was to synthesize Iron Oxide using an eco-friendly method and evaluate the antibacterial effect. Appears to be ecofriendly and cost effective alternative to conventional chemical and physical methods and would be suitable for developing large scale production.

In this study, UV-Vis spectra were carried out for the synthesized nanoparticles. The obtained absorption peaks revealed the presence of nanoparticles in the products. FTIR studies were carried for the prepared nanoparticles and nanocomposites. The vibration frequencies present in the spectra confirmed the formation of the nanoparticles. XRD analyses were carried out for the synthesized nanoparticles and nanocomposites. From the spectrum results, the sizes of the nanoparticles were determined. The calculated values were ranging from 25-100 nm, confirming the nanoscale nature of the products. The morphologies of the synthesized product were studied using SEM analysis. From the SEM images, the shapes of the nanoparticles were observed. The presences of elements in the products were confirmed by EDX analysis.

The antibacterial activity of synthesized Iron Oxide nanoparticles was studied against pathogenic bacteria of gram positive and gram negative strains were compared

with ampicillin, a standard antibacterial agent using agar well-diffusion method. From the results it was seen that the antibacterial activities were found to be good for all concentrations of nanoparticles against the studied pathogens. This green method of synthesizing Fe_3O_4 nanoparticles could also be extended to fabricate other industrially important metal oxides. This simple, low cost and greener method for development of nanoparticles may be valuable in environmental, biotechnological and biomedical applications.

MATERIALS AND METHODS

Collection of Sample

The fresh potato (***Solanum tuberosum*)** was collected from Whole sale market place, Hosur Tamil Nadu state, India during the month of June 2018. The collected potato was identified and authenticated. The collected sample was tightly packed with polyethene bag and then transferred to the laboratory. Then the samples were washed with distilled water twice and kept under room temperature.

Pure Culture

The bacterial strains *Escherichia coli* (NCIM 2065), *Pseudomonas aeruginosa* (NCIM 2036), *Salmonella enterica* (NCIM 5256), *Shigella flexneri* (NCIM 5265), *Staphlococcus aureus* (NCIM 2901), *Vibrio cholerae* (NCIM 5316), *Bacillus cereus* (NCIM 2217), *Listeria monocytogenes* (NCIM 5277), *Proteus mirabilis* (NCIM232), *Klebsiella* sp (NCIM2690) used in this study were obtained from the National Collection of Industrial Microorganisms (NCIM), CSIR – National Chemical Laboratory, Pune, India. They were maintained on nutrient agar slants at 4 °C and were sub cultured every 15 days to maintain its viability.

Method:

Extraction of Magnetic Iron Oxide nonoparticle Fe_3O_4 (Magnetite) nanoparticles were synthesized by co-precipitation method with slight modification as described previously[5]. Briefly, 3gm of FeSO4.7H2O and 6 gm of FeCl3 were dissolved each in 10ml of distilled water separately and the solutions were stirred using magnetic stirrer for 20min. $FeCl_3$ solution was initially sonicated followed by drop wise addition of FeSO4.7H2O solution. This mixture was added to potato extract and the pH of the solution was adjusted to 8 using the 1N NaOH. The resultant black precipitate was allowed to stand for 3 to 4 hrs. without disturbance for the precipitate to settle. The reaction for the formation of iron oxide as $FeSO_4.7H_2O+2FeCl_3 \rightarrow Fe_3O_4+SO\uparrow+6Cl^-+14H^+$. Centrifugation at 5000rpm for 20min was repeated two more times to remove the chlorine contamination and the nanoparticles were finally collected as power after oven dried at 60˚C.

Determination of total phenolic and tannin contents:

The total phenolic content was determined according to the method described by Siddhuraju and Becker[6], the tannin content of the sample was calculated as: Tannin (%) = Total phenolics (%) – Non-tannin phenolics (%).

Estimation of total flavonoid content:

The total flavonoid content of sample extracts was determined by the use of a slightly modified colorimetric method described previously[7]. Absorbance of the mixture was determined at 510 nm versus prepared water blank. Rutin was used as a standard compound for the quantification of total flavonoid. All the values were expressed as gram of rutin equivalent (RE) per 100 gram of extract.

Metal chelating activity*:*

The chelating of ferrous was estimated by the method of Dinis *et al*.[8]. Absorbance of the solution was then measured spectrophotometrically at 562nm. The chelating activity of the extracts was evaluated using EDTA as standard. The results were expressed as mg EDTA equivalent/g extract.

Phosphomolybdenum assay:

The antioxidant activity of samples was evaluated by the green phosphomolybdenum complex formation according to the method of Prieto *et al*.[9]. The absorbance of the mixture was measured at 695nm against a blank. The results reported (Ascorbic acid equivalent antioxidant activity) are mean values expressed as g of ascorbic acid equivalents/ 100g extract.

Assay of superoxide radical scavenging activity:

The assay was evaluated based on the capacity of various extracts to inhibit formazan formation by scavenging the superoxide radicals generated in riboflavin–light–NBT system[10]. The absorbance was measured at 590nm. The percentage inhibition of superoxide anion generation was calculated as: % Inhibition = [(A0 - A1) / A0] X 100, where A0 is the absorbance of the control, and A1 is the absorbance of the sample extract/standard.

Assay of nitric oxide scavenging activity:

The procedure used in the experiment according to the previous study[11]. The absorbance of the chromophore formed was read at 546nm.

Hydrogen peroxide scavenging activity:

The ability of the extracts to scavenge hydrogen peroxide was determined according to the method of Ruch *et al*.[12] Absorbance of hydrogen peroxide at 230nm was determined, the percentage inhibition activity was calculated from [(A0 - A1)/A0] X100, where A0 is the absorbance of the control (reaction mixture without extract) and A1 is the absorbance of the extract/standard.

Hydroxyl radical scavenging activity:

The scavenging activity of chloroform, acetone, methanol and hot water extracts of H. herbacea and N. alata on hydroxyl radical was measured according to the method of Klein *et al* [13]. The intensity of the color formed was measured spectroscopically at 412nm against reagent blank. The % hydroxyl radical scavenging activity (HRSA) is calculated by: % HRSA = from [(A0 - A1)/A0] X100, where A0 is the absorbance of the control and A1 is the absorbance of the extract/standard.

Free radical scavenging activity on DPPH•:

The antioxidant activity of the extracts was determined in terms of hydrogen donating or radical scavenging ability using the stable radical DPPH, according to the method of Blios[14]. The absorbance of the sample was measured at 517nm. Radical scavenging activity was expressed as the inhibition percentage of free radical by the sample and was calculated by: % DPPH radical scavenging activity = (Control OD – Sample OD / Control OD) X 100.

Micro biological tests:

The standard microbiological tests such as Gram's staining followed by Morphological characterization and biochemical characterization tests such as Carbohydrate fermentation test, Starch utilization, Catalase test, Voges - Proskauer test, Urease test, Oxidase test, Gelatin liquefaction and Motility test were performed to identify the organism[15].

Antibacterial assay:

The standard antibacterial assays such as Agar well diffusion method[16], Antimicrobial screening by disk diffusion technique[17], Minimal Inhibitory Concentration (MIC) (Broth Tube Dilution Method) were performed.

Characterization of the Synthesized Iron Oxide Nanoparticles:

UV – Vis Spectroscopy:

Ultraviolet-visible spectroscopy (UV-Vis) means absorption of spectroscopy in the UV-visible spectral region. The iron nanoparticles were characterized by UV-VIS absorption spectrum and recorded in the region 190-1100nm using a Perkin Elmer (Model: Lambda 35, path length of 1.0cm, scan rate 1920nm/sec) UV-Vis-NIR Spectrometer. The double distilled water was used as a blank reference.

Fourier Transform Infra-Red Spectroscopy (FTIR):

The nanoparticles were distinguished using a Fourier Transform Infrared Spectrophotometer (Perkin Elmer RX1 and Nicolet Avatar Model spectrophotometers). Two milligrams of the sample were mixed with 100mg Potassium bromide (KBr). Then, condensed to prepare a salt disc approximately 3mm in diameter and the disc were directly kept in the sample holder. FTIR spectra were verified in the absorption range between 400 and 4000cm^{-1}.

X-Ray Diffraction (XRD) Analysis:

The particle size and nature of the silver nanoparticles were found out using XRD. XRD patterns were recorded with a PANalytical Philips X'Pert ProX-ray diffractometer Using CuKα radiation (λ= 1.5406 Å) low angle diffract grams were recorded in the 2θ range 5.0 - 80° with a 2θ step size of 0.02° and a step time of 20 second at each point. X-ray powder diffraction is a rapid analytical technique mainly used for phase classification of a crystalline material and can supply information on unit cell dimensions. The analyzed material is finely ground, and the mean bulk composition is found out. The particle or grain size of the particles on the iron nanoparticles was determined using Debye Sherrer's equation.

$$D = 0.94\,\lambda / B \cos\theta$$

X-ray analyser (EDAX)

The elemental analysis was examined by energy dispersive X-ray analyser (EDAX) system (Model: Oxford INCA Penta FET X3) and HPLC, LC-2030 3D model (Low pressure quaternary gradient system) was used with inbuilt PDA detector. Shimadzu lab solutions software (ver. 5.8) was used to operate the HPLC.

Scanning Electron Microscope (SEM) analysis:

The surface morphologies were characterized by SEM using JEOL JSM-6390 and FEI Quanta 200 scanning electron microscopes at an accelerating voltage of 20keV. SEM is a kind of electron microscope that projects a sample by scanning it with a tall energy beam of electrons in a faster scan patterns. This film of the sample was arranged on a carbon coated copper grid by immediately dropping a very small amount of the sample on the grid. Extra solution was removed by means of a blotting paper and then the films on the SEM grid were permitted to dry by putting it under a mercury lamp for 5min. Areas ranging from approximately 1cm to 5 microns in width can be imaged in a scanning mode using conventional SEM techniques (magnifications ranging from 20X to approximately 30,000X with spatial resolution of 50 to 100 nm).

RESULTS AND DISCUSSION

Nanoparticles characterization is important to comprehend and succeed the nanoparticles synthesis and applications. Characterization is attained by using various techniques such as Scanning and Transmission, UU-vis spectroscopy (UV-Vis), powder X-ray diffractometry (XRD), Fourier Transform Infrared spectroscopy (FTIR), and Electron Microscopy (SEM)[17-22]. These techniques are used for determination of different parameters such as particle range, character crystallinity, fractal dimensions, pore size and surface area. Recently, investigators have paid more consideration on the green synthesis and applications of Iron Oxide using various plant extracts. The present study was carried out to the synthesis Iron Oxide using aqueous extract of *Solanum tuberosum*.

Synthesis of Iron Oxide-Nanoparticles (Visual Inspection)

In the typical synthesis of iron oxide nanoparticles, *Solanum tuberosum* extract was added slowly into FeCl3 solution at room temperature. After adding the leaf extract into $FeCl_3$ solution, within 3min, a visible color change was observed, the yellow color aqueous solution of FeCl3 turned to greenish black indicating the synthesis of Iron oxide nanoparticles (Fig 1).

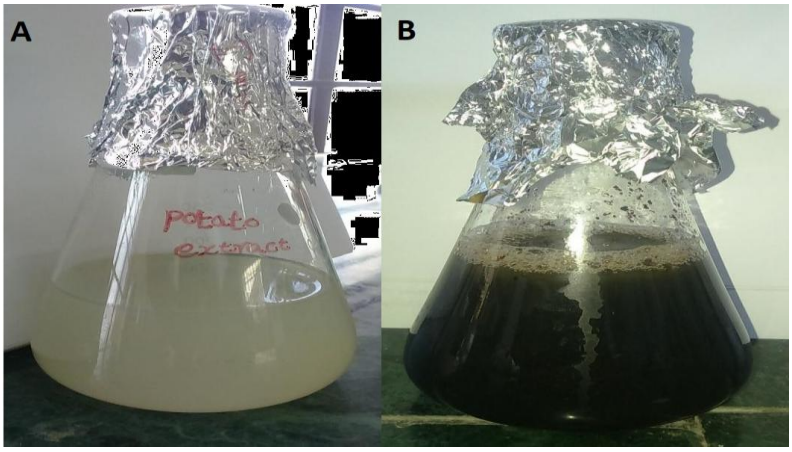

Figure 1: Synthesis of Iron Oxide Nanoparticles (Visual Inspection):

(A) before nanoparticle synthesis, (B) after nanoparticle synthesis.

Antioxidant activity of *Solanum tuberosum* extracts

The results of Antioxidant activity of *Solanum tuberosum* depicted in the represented Tables 1 to 8.

Table 1: Total phenolics, tannin and flavonoid contents in hot water extracts of *S. tuberosum*

Concentration of the sample (µg/ml)	Total phenolics (mg GAE / gm extract)	Tannin (mg GAE/ gm extract)	Total Flavonoids (mg RE / gm extract)
10	50.48	35.24	310.67
20	56.67	83.33	314.00
30	62.38	83.33	331.33
40	25.24	138.57	346.00
50	85.24	122.86	381.33
60	100.48	256.19	408.67
70	108.10	281.43	436.00
80	115.24	293.81	452.00
90	117.14	327.14	526.00
100	124.29	332.38	593.33

GAE; Gallic acid equivalent, RE; Rutin equivalent.

Table 2: Total phenolics, tannin and flavonoid contents in acetone extracts of *Solanum tuberosum*

Concentration of the sample (µg/ml)	Total phenolics (mg GAE / gm extract)	Tannin (mg GAE/ gm extract)	Total Flavonoids (mg RE / gm extract)
10	45.71	21.90	12.67
20	68.10	24.29	37.33
30	92.86	34.29	80.00
40	110.95	73.33	82.00
50	100.48	99.05	147.33
60	119.52	99.52	280.67
70	147.14	138.57	296.00
80	171.90	158.10	298.00
90	177.14	198.10	318.67
100	196.19	389.52	332.00

GAE; Gallic acid equivalent, RE; Rutin equivalent.

Table 3: Metal chelating, Phosphomolybdenum and super oxide radical scavenging activity of hot water extracts of *Solanum tuberosum*

Concentration of the sample (µg/ml)	Metal chelating activity (mg EDTAE / gm extract)	Phosphomolybdenum activity (mg AAE/ gm extract)	Superoxide Radical Scavenging (%)
10	NR	10.89	49.57
20	NR	44.89	54.61
30	NR	47.28	58.97
40	1.31	48.11	60.87
50	10.38	53.89	64.67
60	10.48	54.89	70.47
70	14.10	63.56	79.96
80	15.03	69.83	81.39
90	19.59	72.67	86.61
100	23.34	74.83	91.36

EDTAE: Ethylene diamine tetra acetic acid equivalent;

AAE: Ascorbic acid equivalent.

Table 4: Metal chelating, Phosphomolybdenum and super oxide radical scavenging activity of acetone extracts of *Solanum tuberosum*

Concentration of the sample (µg/ml)	Metal chelating activity (mg EDTA / gm extract)	Phosphomolybdenum activity (mg AAE/ gm extract)	Superoxide Radical Scavenging (%)
10	NR	6.00	53.28
20	NR	18.17	55.18
30	NR	18.67	63.06
40	NR	25.89	67.90
50	NR	31.61	71.60
60	0.90	38.44	78.06
70	3.90	39.50	81.67
80	10.17	42.89	86.13
90	15.55	49.50	88.51
100	17.45	50.06	90.31

EDTAE: Ethylene diamine tetra acetic acid equivalent; AAE: Ascorbic acid equivalent.

Table 5: Nitric Oxide Scavenging, Hydrogen Peroxide Scavenging and Hydroxyl Radical Scavenging activity of hot water extracts of *Solanum tuberosum*

Concentration of the sample (µg/ml)	Nitric Oxide Scavenging (%)	Hydrogen Peroxide Scavenging (%)	Hydroxyl Radical Scavenging (%)
10	43.97	NR	32.10
20	52.04	NR	32.57
30	53.66	8.45	37.13
40	58.31	13.39	40.55
50	64.48	17.66	41.79
60	74.07	23.17	44.06
70	78.44	26.21	45.30
80	81.48	28.58	51.38
90	89.84	33.90	53.28
100	99.05	36.37	59.07

Table 6: Nitric Oxide Scavenging, Hydrogen Peroxide Scavenging and Hydroxyl Radical Scavenging activity of acetone extracts of *Solanum tuberosum*

Concentration of the sample (µg/ml)	Nitric Oxide Scavenging (%)	Hydrogen Peroxide Scavenging (%)	Hydroxyl Radical Scavenging (%)
10	43.30	3.61	53.85
20	47.58	5.22	60.87
30	52.61	10.07	65.24
40	56.60	13.30	70.56
50	61.92	15.29	71.60
60	63.82	17.76	79.49
70	65.43	19.09	80.15
80	73.03	22.60	83.67
90	78.73	25.74	86.42
100	83.76	29.15	86.51

Table 7: DPPH Scavenging activity of hot water extracts of *Solanum tuberosum*

Concentration of the sample(µg/ml)	DPPH Scavenging (%)
10	31.13
20	36.71
30	38.88
40	40.23
50	41.37
60	47.05
70	48.40
80	49.33
90	49.74
100	49.84

Table 8: DPPH Scavenging activity of acetone extracts of *Solanum tuberosum*

Concentration of the sample(µg/ml)	DPPH Scavenging (%)
10	12.00
20	17.48
30	32.16
40	38.06
50	40.95
60	43.74
70	45.09
80	49.95
90	49.95
100	49.95

Antibacterial assay[23]

Antibacterial activity of Iron oxide nanoparticles: Agar well diffusion method

The antibacterial properties of the Iron Oxide Nanoparticles were evaluated against Gram positive and Gram negative bacterial strains using agar well diffusion method. Table 9 shows the effect of Iron oxide nanoparticles on the growth of both Gram positive and Gram negative bacteria. Iron oxide nanoparticles exhibited significant antibacterial activity against Gram positive bacteria than Gram negative pathogenic bacterial strains tested.

Of the bacterial stains tested, Iron oxide nanoparticles strongly inhibited the growth of Gram positive bacteria - *Bacillus cereus (*10mm*)*, *Staphylococcus aureus* (20mm) and *Listeria monocytogens* (16mm) at a concentration of 150µg. On the other hand, Iron oxide nanoparticles moderately inhibited the growth of Gram negative bacteria- *Escherichia coli* (10mm) and *Klebsiella pneumoniae* (10mm), *Proteus mirabilis* (11mm), *Salmonella enterica* (19mm), *Shigella flexneri* (2mm), *Vibrio cholerae* (10mm) and *Pseudomonas aeuroginosa* (20mm) at a concentration of 150µg. These nanoparticles showed a low inhibitory effect on the growth of *Bacillus cereus* (10mm).

Table 9: Antibacterial activity of Iron oxide nanoparticles by Agar well diffusion method

Bacterial strain	Zone of inhibition (Well method)											
	Iron oxide nanoparticle								Ampicillin			
	10µg	20µg	30µg	50µg	50µg	80µg	100µg	150µg	10µg	20µg	30µg	50µg
Staphylococcus aureus	_	_	_	_	_	_	_	10mm	15mm	17mm	18mm	20mm
Bacillus subtilis	_	_	_	_	_	10mm	10mm	10mm	10mm	10mm	10mm	10mm
Listeria monocytogens	10mm		10mm	10mm	10mm	10mm	10mm	10mm	12mm	13mm	15mm	16mm
Escherichia coli	10mm	10mm	10mm	10mm	10mm	10mm	10mm	10mm	14mm	16mm	19mm	21mm
Proteus valgauries	_	_	_	_	_	_	_	11mm	10mm	11mm	12mm	14mm
Klebsiella pneumonia	10mm	10mm	10mm	10mm	10mm	10mm	10mm	10mm	14mm	15mm	17mm	19mm
Salmonella typhimurium	_	_	_	_	_	_	15mm	19mm	17mm	19mm	21mm	23mm
Shigella dysenteriae	_	_	_	_	_	15mm	19mm	22mm	_	_	_	_
Vibrio cholerae	_	_	_	_	_	_	_	10mm	16mm	17mm	19mm	20mm

Antimicrobial screening by disk diffusion technique

Antibacterial activity results of *Solanum tuberosum extract* were given in the Table 10. In general, the mean zone of inhibition produced by the commercial antibiotic, ampicillin, was between 10.0 to 13.0mm and was larger than those produced by *Solanum tuberosum* extracts which was between 10.0 - 13mm. *Bacillus cereus (No zone formation)*, *Staphylococcus aureus* (12mm) and *Listeria monocytogens* (10mm) at a concentration of 150µg. On the other hand, Iron oxide nanoparticles moderately inhibited the growth of Gram negative bacteria- *Escherichia coli* (10mm) and *Klebsiella pneumoniae* (10mm), *Proteus mirabilis* (10mm), *Salmonella enterica* (10mm), *Shigella flexneri* (10mm), *Vibrio cholerae* (10mm) and *Pseudomonas aeuroginosa* (10mm) *at* a concentration of 50µg. These nanoparticles showed a low inhibitory effect on the growth of *Bacillus cereus (No zone formation)*.

Table 10: Antibacterial activity of Iron oxide nanoparticles by disk diffusion technique

Bacterial Strain	Zone of inhibition (diameter in mm) Disc method				
	Iron oxide nanoparticle				Ampicillin
	10µg	20µg	30µg	40µg	Antibiotic disc
Staphylococcus aureus	_	_	_	10	10
Bacillus cereus	_	_	_	10	_
Listeria monocytogens	_	_	_	10	10
Escherichia coli	_	_	_	10	10
Proteus mirabilis	_	_	_	10	10
Klebsiella pneumonia	_	_	_	10	_
Salmonella enterica	_	_	_	10	10
Shigella flexneria	_	_	_	10	10
Vibrio cholerae	_	_	_	10	13
Pseudomonas aeruginosa	_	_	_	_	_

Minimal Inhibitory Concentration (MIC)

(Broth Tube Dilution Method)

Minimum inhibitory concentration of Iron Oxide Nanoparticles for the antibacterial activities was presented in the Table 11. The Minimal Inhibitory Concentration produced by the commercial antibiotic, ampicillin, was between 500 µg and was larger than those produced by extracts which was between 500 – 2000 µg[23].

Bacterial strains were spread on agar plates. Different amounts of Fe_3O_4 nanoparticles (25µg and 50µg) were placed in the wells. Controls contained Ampicillin (20µg) in place of Fe_3O_4 nanoparticles. The incubation period was 24 h at 37°C. Zone of inhibition was measured as described in methods.

Bacterial strains were spread on agar plates. Different concentrations of Iron oxide nanoparticles (0.1-2.0 mg/ml) were placed in the wells. Control contained Ampicillin (20µg) in the place of nanoparticles. The incubation period was 24 h at 37ºC. Zone of inhibition was measured and minimum inhibitory concentration of Iron oxide nanoparticles was determined.

Table 11: Antibacterial activity of Iron oxide nanoparticles by Minimal Inhibitory Concentration (Broth Tube Dilution Method)

Name of the bacteria	Minimum inhibitory concentration (MIC) of iron oxide nanoparticles (µg/ml)	Ampicillin
Staphylococcus aureus	1000	500
Bacillus cereus	500	500
Listeria monocytogens	1500	500
Escherichia coli	2000	500
Proteus mirabilis	1000	500
Klebsiella pneumonia	500	500
Salmonella enterica	2000	500
Shigella flexinaria	1500	500
Vibrio cholerae	1000	500
Pseudomonas aeuroginosa	500	500

Synthesis of Iron Oxide-Nanoparticles (Visual Inspection)

Generally, the iron oxide nanoparticles have been prepared by strong hydrolysis of iron salts at elevated temperature[24]. The plant mediated iron oxide nanoparticles were prepared at room temperature. Hence the mechanism of study of iron oxide nanoparticles formation is a little difficult. However, the organic compound, which is present in the plant extract, acts as a reducing as well as capping or binding agent to form iron oxide nanoparticles. The colour change arise from the excitation of the surface plasman resonance (SPR) phenomenon is typically of iron oxide nanoparticles[23,25].

Characterization of Iron Oxide nanoparticles UV-vis spectroscopic analysis:

The optical property of synthesized iron oxide nanoparticles is one of the important characteristics for evaluation of its optical and photo catalytic activity. UV-Visible absorption spectrum is the preliminary characterization to know the optical property. The result obtained from UV-Visible spectroscopy analysis of the sample is presented in Fig 2.

Addition of *Solanum tuberosum* extract to 0.001 M ferric (III) chloride produced an instantaneous color change in the solution from yellow to intense brown, indicating the formation of iron-containing nanoparticles[26]. This phenotypic change correlated well with the absorption spectra data, such that the absorption peak at 360 nm of the ferric (III) chloride was shifted to 405 nm after the addition of the plant extract, with the 405 nm peak being indicative of iron nanoparticle formation.

In the present study, the absorption maxima of synthesized Iron oxide nanoparticles are similar to those observed in other studies which used tea and sorghum extracts to produce iron nanoparticles[26-28]. An absorption maxima of iron nanoparticles with a peak of 415 nm has been reported[29-30].

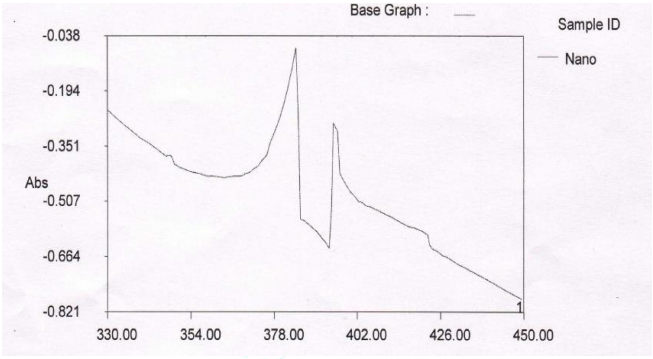

Figure 2: UV-Vis analysis of synthesized Iron Oxide nanoparticles of *Solanum tuberosum*

Fourier Transform Infrared Spectroscopy (FTIR):

FTIR spectra of biosynthesized Iron oxide nanoparticles were recorded to identify the capping and efficient stabilization of metal nanoparticles by functional groups of biomolecules present in *Solanum tuberosum extract* leaf extract. Fig 3 shows the FT-IR spectrum of prepared iron oxide nanoparticles. It displays three strong bands around 3468 cm^{-1}(br), 1626 cm^{-1} and 548 cm^{-1}. The observed bands are nearer to those reported for Iron nanoparticles[31]. The vibration bands are 615 cm^{-1} (Fe–O stretching), 1632 cm^{-1} (H_2O bending vibration) and a broad peak at 3424cm^{-1} (H_2O stretching) indicating phenolic compounds. Presence of organic molecule on the surface of iron oxide nanoparticles has the influence on the FT-IR peaks[32]. The broad peak observed around 548 cm^{-1} (Fe–O stretching) instead of two sharp peaks, may be due to the organic molecule which was from the leaf extract on the surface of iron oxide nanoparticles. The weak band at 2074 cm^{-1} may be due to the unsaturated Nitrogen (C≡N) compounds, tannins and alkaloids from the leaf extract. Based on these results, the presence of phenolic compounds, tannins and alkaloids were believed to be responsible for the formation and stabilization of synthesized iron oxide nanoparticles.

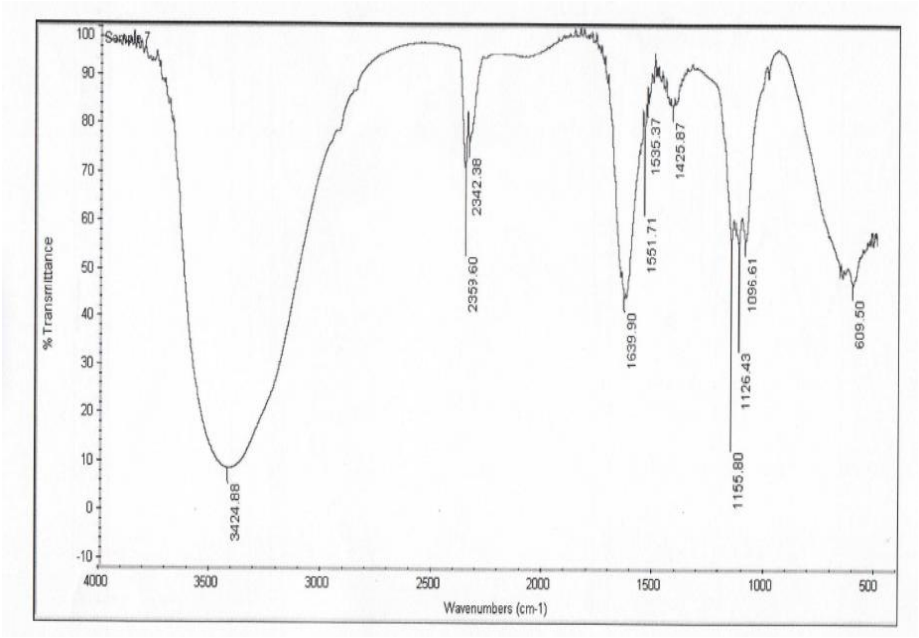

Figure 3: FT-IR spectra of synthesized Iron Oxide nanoparticles of *Solanum tuberosum*

X-ray Diffractometry (XRD) analysis:

The phase identification and crystalline structure of the nanoparticles were characterized by X-ray diffraction. The X-ray diffraction patterns obtained for the Fe_3O_4 - NPs synthesized using *Solanum tuberosum extract* extract is shown in Fig 4. The synthesized particles when subjected to XRD analysis, gave a clear picture on the presence of major characteristic peaks for prepared crystalline metallic nanoparticles at 2θ values of 22.1, 31.0, 33.5, 38.7, 47.2, 52.6, 55.4, 60.4, and 62.8 degrees corresponding to (14), (102), (112), (115), (21), (113), (012), (218), and (298) respectively. In addition, the peak observed at 2θ values of 44.9 is corresponding to (335). It might be due to the presence of trace amount of hollow –Fe_3O_4 nanoparticles. It indicates that the prepared iron oxide nanoparticles are well crystalline. Above all, it is encouraging to note that the 2θ values of the synthesized iron oxide nanoparticles are also matched with Joint Committee for Powder Diffraction Standard (JCPDS) which are in rhombohedral geometry. The average particle size calculated from XRD increased with an increase in temperature and time. Based on the cocercivity, it was concluded that the nanoparticles were superparamagnetic in nature.

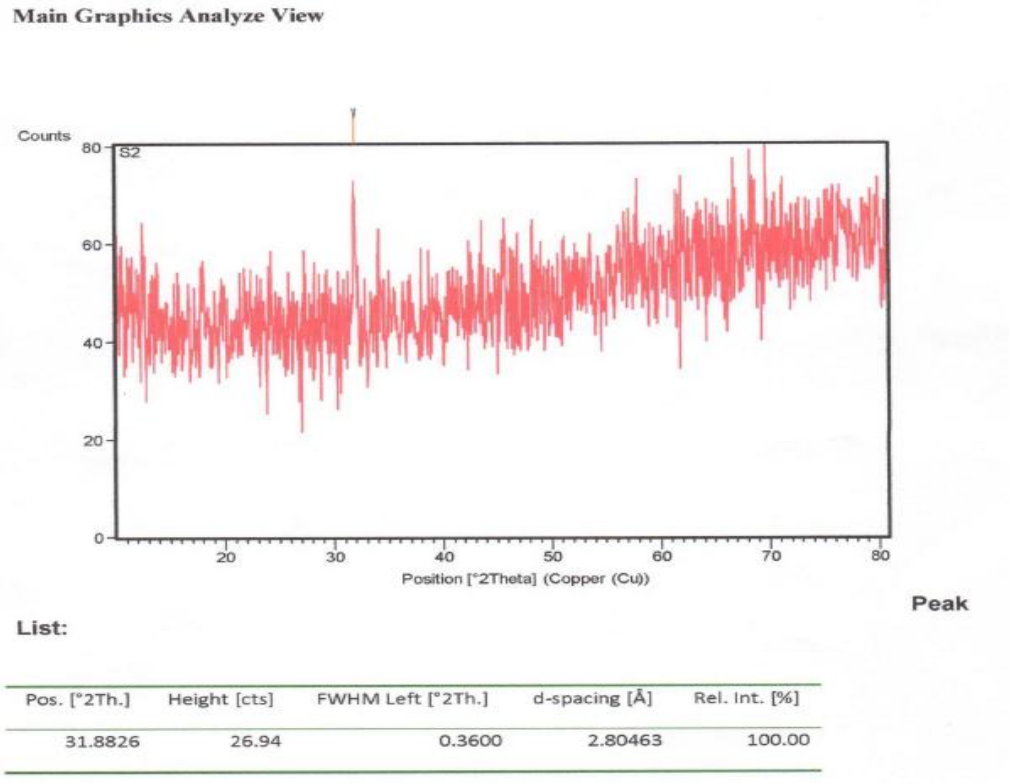

Figure 4: XRD analysis of synthesized silver nanoparticles of *S. tuberosum*

SEM and EDX analysis:

SEM images revealed that the synthesized iron oxide nanoparticles were aggregated as irregular rhombic shapes with panoramic view and range from 105-145 nm in size (Fig 5a to 5d). To find out the purity of the metal particles synthesized, EDX spectrum was obtained. Dispersive X- ray Spectroscope (EDX) analysis showed the presence of elemental iron oxide signal in the sample. The appearance of chloride and carbon in the EDX spectrum is because of the FeCl3 precursors used in the synthesis protocol and attributed mainly to organic molecules in the extract. Iron oxide nanoparticles synthesized by using *Solanum tuberosum* showed that the synthesized nanoparticles were plate like structures with coarsened grains, uniformly distributed small spherical shaped particles and at higher magnification, large number of homogeneous nanocapsule like morphology of iron oxide nanoparticles were observed. In the previous studies reported that the typical SEM image revealed that the iron nanoparticles were clearly distinguishable at different enlargements were found to be polydispersed and measured in size from 24 to 34 nm.

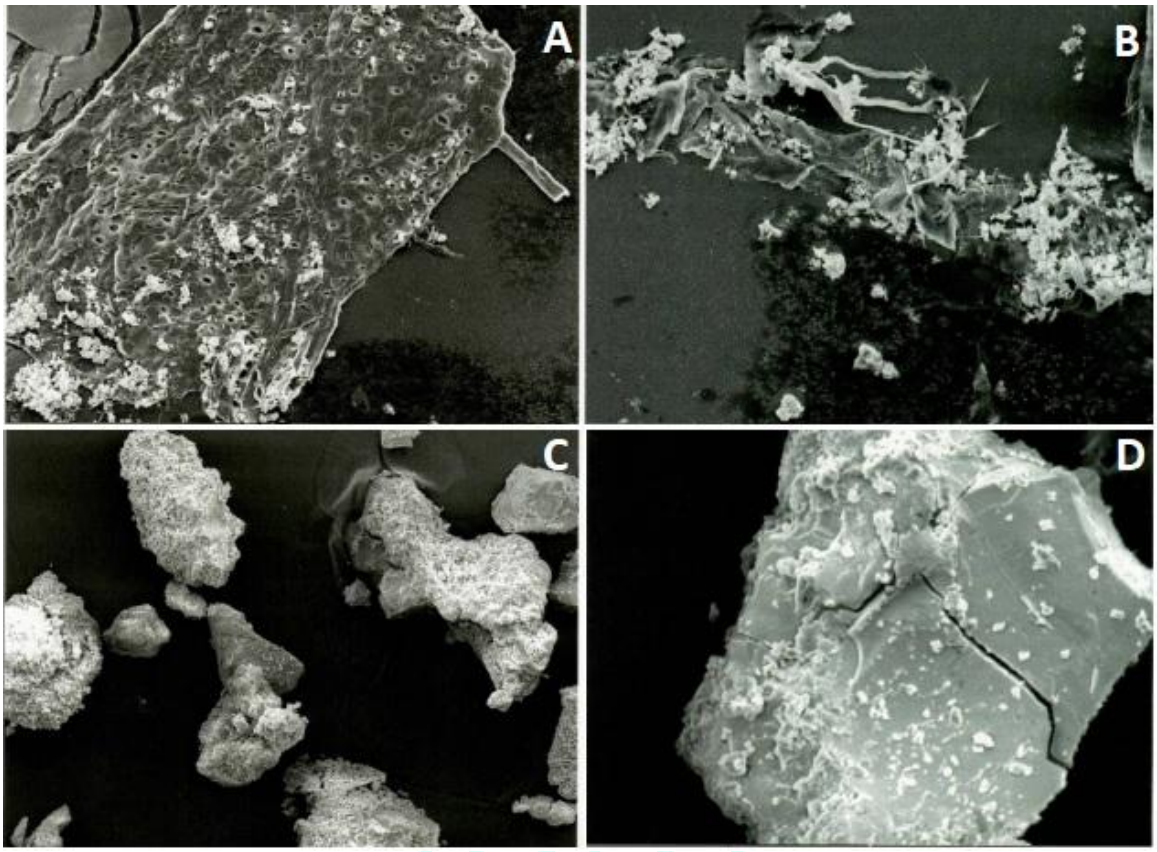

Figure 5: SEM images of Iron Oxide nanoparticles synthesized using *Solanum tuberosum* at different magnification levels. Fig 8A to 8D: SEM HV 10.0Kv; SEM MAG 951x, 1.85kx, 643x, 1.76kx;

View field 201µm, 103µm, 297µm, 109µm and WD 47.19mm, 45.78mm, 47.24mm, 47.24mm correspondingly.

High performance liquid chromatography (HPLC) analysis:

The optimization of extraction conditions for HPLC method can be used to develop a fingerprint for the identification of *Solanum tuberosum extract* leaf extract (Table 9). It is revealed from Table 9 that in 10 µL of *Solanum tuberosum* extract, there are 11 peaks at the Rt 0.429, 4.17, 4.482, 4.948, 5.285, 7.418, 8.138, 8.308, 8.981, 11.89 and 13.12 as shown in Fig 6, indicating the occurrence of at least 11 different components in 10 µL *Solanum tuberosum* extract.

Table 9: HPLC pattern of synthesized Iron Oxide of *S. tuberosum* extract

ID	RT	Height	Area	Conc	Half Width	Theo Plate	Tail Fact
1	0.429	29	462.3	0.6929	15.94	14.4	1
2	4.17	420	8542.7	12.8044	20.34	837.73	0.83
3	4.482	362	4291.1	6.4318	11.85	2848.83	1.44
4	4.948	107	2366.2	3.5466	22.11	997.96	0.78
5	5.285	190	5210.5	7.8098	27.42	740.16	2.72
6	7.418	3	198.4	0.2974	66.15	250.66	0.69
7	8.138	15	249.4	0.3738	16.62	4776.67	0.65
8	8.308	13	112.5	0.1686	8.65	18372.12	1.16
9	8.981	543	9040.4	13.5505	16.65	5800	1.08
10	11.89	26	846.3	1.2685	32.55	2660.27	0.82
11	13.12	1637	35397	53.0558	21.62	7331.96	1.01

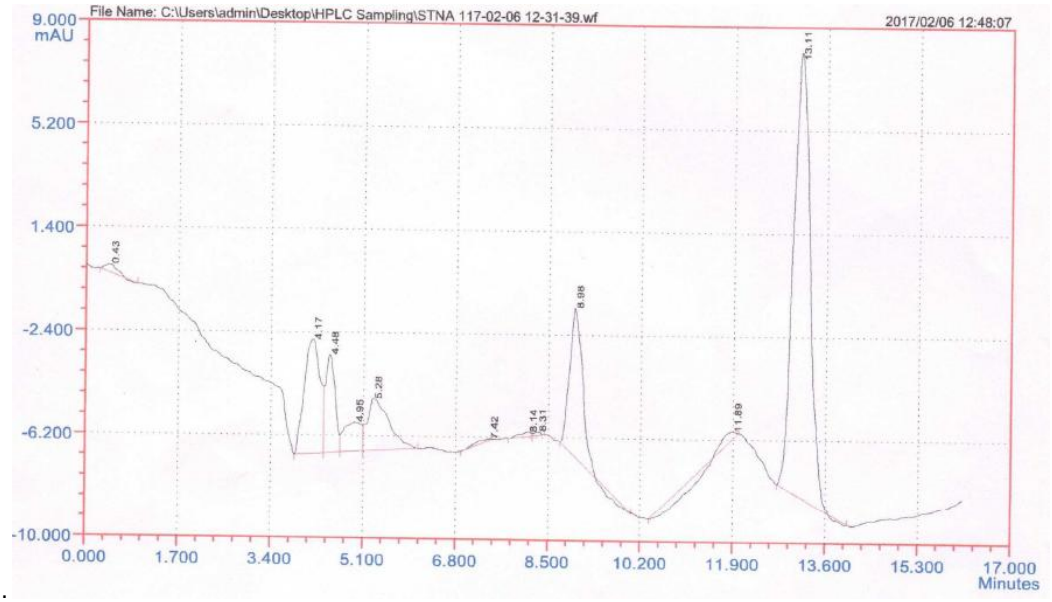

Figure 6: HPLC pattern of Iron Oxide synthesized using *Solanum tuberosum* extract

CONCLUSION

In conclusion, environmentally benign and low cost synthesis of Iron Oxide nanoparticles can be achieved using the extract of *Solanum tuberosum*. The synthesized Iron oxide nanoparticles good antibacterial activity against gram positive pathogens *Bacillus cereusmm*, *Staphylococcus aureus* and *Listeria monocytogenes,* and moderate antibacterial activity against gram negative bacteria pathogens *Escherichia coli, Klebsiella pneumoniae*, *Proteus mirabilis*, *Salmonella enterica*, *Shigella flexneri*, *Vibrio cholerae* and *Pseudomonas aeuroginosa.* Therefore, nanoparticles of Iron Oxide in combination with commercial available antibiotics could be used as an antibacterial agent after further trails on experimental animals.

REFERENCES

1. Mohanpuria P, Rana NK, Yadav SK. Biosynthesis of nanoparticles, technological concepts and future applications. Journal of Nanoparticle Research. 2007; 10:507-517.
2. Thakkar KN, Mahatra SS, Parikh RK. Biological synthesis of metallic nanoparticles. Nanomadicine and Nanotechnology. 2010; 6:257-262.
3. Sharma VK, Yngard RA, Lim, Y. Silver nanoparticles green synthesis and their antimicrobial activities. Advances Colloid Interface Science. 2008; 145:83-96.
4. Celeste M. Raker and David M. Spooner. Chilean tetraploid cultivated potato, Solanum tuberosum is distinct from the andean populations: Microsatellite Data, University of Wisconsin, published in Crop Science. 2002; Vol.42.
5. Panigrahi S, Kundu S, Ghosh SK, Nath S, Pal T. General method of synthesis for metal nanoparticles. Journal of Nanoparticle Research. 2004; 6(4):411–414.
6. Siddhuraju P, Becker K. Antioxidant properties of various solvent extracts of total phenolic constituents from three different agroclimatic origins of drumstick tree (Moringaoleifera Lam.) leaves. Journal of Agricultural and Food Chemistry. 2003; 51 (8):2144-2155.
7. Zhishen J, Mengcheng T and Jianming W. The determi- nation of flavonoid contents in mulberry and their scavenging effects on superoxide radicals. Food Chemistry, 1999; 64:555 -559.
8. Dinis TCP, Madeira VMC, Almeida MLM. Action of phenolic derivates (acetoaminophen, salycilate and 5-aminosalycilate) as inhibitors of membrane lipid peroxidation and as peroxyl radical scavengers. Archives of Biochemistry and Biophysics. 1994; 315:161-169.
9. Prieto P, Pineda M and Aguilar M. Spectrophotometric quantitation of antioxidant capacity through the formation of a Phosphomolybdenum Complex: Specific application to the determination of vitamin E. Analytical Biochemistry. 1999; 269:337-341.
10. Beauchamp C and Fridovich I. Superoxide Dismutase: Improved Assays and an Assay Applicable to Acrylamide Gels. Analytical Biochemistry. 1971; 44:276-287.
11. Sreejayan N and Rao MNA. Nitric oxide scavenging activity by curcuminoids. Journal of Pharmacy and Pharmacology. 1997; 47:105-107.
12. Ruch, RJ, Cheng SJ, and Klaunig JE. Prevention of cytotoxicity and inhibition of intracellular communication by antioxidant catechins isolated from Chinese green tea. Carcinogenesis. 1989; 10:1003-1008.
13. Klein SM, Cohen G, Cederbaum AI. Production of formaldehyde during metabolism of dimethyl sulphoxide by hydroxyl radical generating system. Biochemistry. 1991; 20:6006- 601.
14. Blois MS. Antioxidant determinations by the use of a stable free radical. Nature. 1958; 29:1199 - 1200.
15. Gunasekaran P. Laboratory Manual in Microbiology. New Age International Pvt. Ltd. Publishers, New Delhi. 1995.
16. Murray PR, Baron EJ, Pfaller MA, Tenover FC, Yolken HR. Manual of Clinical Microbiology. 6th Ed. ASM Press, Washington DC, 1995; 15-18.
17. NCCLS. Methods for dilution antimicrobial susceptibility tests for bacteria that grow aerobically. 3rd ed. Wayne, PA: NCCLS; 2002; M100-S12.
18. Hulther E, Fendler JH. Explostation of localized surface plasmon resonance. Advances Materials. 2004; 16:1688-1706.
19. Sun S, Murray C, Weller D, Folks L, Mosar. Monodisperse Fe pt nanoparticles and ferromagnetic Fe pt nanocrystal superlattices. Science. 2000; 267:1989-1992.
20. Vilchis-Nestor AR, Sanchez–Mendieta V, Camacho–Lopaz MA, Comez–Espinosa RM, Camacho-Lopez MA, Arenas–Alatorre JA. Solventless synthesis and opticle properties of Au & Ag nanoparticles using Camellia sinensis extract. Materials Letters. 2008; 67:3103-3105.
21. Zhang W, Qiao X, Chem J, Wany H. Preparation of silver nanoparticles in waher in oil AOT reverse micelles. Journal of Colloidal Interface Science. 2006; 302:170-173.
22. Chimentao RJ, Kirm I, Medina F, Rodriguez X, Cesteros Y, Salagre P, Sueiras JE. Different morpholopies of silver nanoparticles as catalysts for the selective oxidation of styrene in the gas phase. Chemical Communication. 2004; 4:846-847.
23. Veeramanikandan V, Madhu G, Pavithra V, Jaianand K and Balaji P. Green Synthesis, Characterization of Iron Oxide Nanoparticles using Leucas Aspera Leaf Extract and Evaluation of Antibacterial and Antioxidant Studies. International Journal of Agriculture Innovations and Research. 2017; 06(02):242-250.
24. Ocana M, Morales MP, Serna CJ. Homogeneous precipitation of uniform α-Fe2O3 particles from iron salts solutions in the

presence of urea. Advances in Colloid and Interface Science. 1999; 212 (2):317-323.
25. Shankar SS, Rai A, Ankamwar B, Singh A, Ahmad A, Sastry M. Biological synthesis of triangular gold nanoprisms. Nature Materials. 2004; 3(7):482-488.
26. Kharissova OV, Dias HV, Kharisov BI, Perez, BO, Perez VM. The greener synthesis of nanoparticles. Trends Biotechnology. 2013; 31(4):240–248.
27. Njagi EC, Huang H, Stafford L, Genuino H, Galindo HM, Collins J, Hoag GE, Suib SL. Biosynthesis of iron and silver nanoparticles at room temperature using aqueous sorghum bran extracts. Langmuir. 2011; 27(1):264-271.
28. Hoag G, Collins A, Holcomb J, Hoag J, Nadagouda M, Varma R. Degradation of bromothymol blue by 'greener' nano-scale zero-valent iron synthesized using tea polyphenols. Journal of Materials Chemistry. 2009; 19:8671–8677.
29. Madhavi V, Prasad T, Reddy AVB, Ravindra Reddy B, Madhavi G. Application of phytogenic zerovalent iron nanoparticles in the adsorption of hexavalent chromium. Spectrochimica Acta, Part A: Molecular and Biomolecular Spectroscopy. 2013; 116:17–25.
30. Mazur M, Barras A, Kuncser V. Iron oxide magnetic nanoparticles with versatile surface functions based on dopamine anchors. Nanoscale. 2013; 5:2692–2702.
31. Kumar A, Singhal A. Synthesis of colloidal β-Fe2O3 nanostructures-influence of addition of Co2+ on their morphology and magnetic behavior. Nanotechnology. 2007; 18(47):1-7.
32. Lee J, Tetsuhiko I, Mamoru S. Preparation of ultrafine Fe3O4 particles by precipitation in the presence of PVA at high pH. Journal of Colloid and Interface Science. 1996; 177(2):490-494.